Structural and Electrical Characterization of the Series $La_{1.33}Na_xMn_xTi_{2-x}O_6$

Ana Isabel Ruiz,[a] María Luisa López,*[a] María Luisa Veiga,[a] and Carlos Pico[a]

Dedicated to Prof. Gaitán on the occasion of his 70th birthday

Keywords: Perovskite phases / Mixed conductors / Materials science / Neutron diffraction / X-ray diffraction

A new series of perovskite-type materials of general formula $La_{1.33}Na_xMn_xTi_{2-x}O_6$ (x = 0.66, 0.55 and 0.44) was obtained and characterized. The common structure is rhombohedral (space group $R\bar{3}c$) although a transition to orthorhombic (space group *Ibmm*) is observed between 400 and 600 K for the x = 0.66 phase. Complex impedance techniques and charge/discharge cycles show a different electrical behavior that varies from a purely electronic conductor (x = 0.66) to a mixed electronic-ionic behavior for the other phases.

Introduction

Complex oxides with a perovskite or perovskite-type structure offer a wide range of interesting electrical properties, e.g. giant magnetoresistance, superconductivity and fast ion conductivity. In this context, complex oxides showing ion-electron conducting properties have received much attention due to their use as electrode materials in solid state batteries.

Perovskite-type oxides based on elements of the first transition series display a wide variety of defect-related phenomena which have their origin in the unfilled 3d electron shell. The relative ease with which electrons can be removed from or added to some metal cations, especially Fe and Mn, means that they often exist in different valence states, depending on the temperature and oxygen partial pressure. This fact also gives rise to a potentially large number of phases, which themselves may deviate from exact stoichiometry in terms of both cation and oxygen contents.[1] On the other hand, defects in perovskite oxides can arise from cation deficiency and the resulting vacancies often form ordered superstructures.

Among the mixed oxides with the perovskite structure, those containing Mn cations have recently attracted a great deal of interest due to their giant negative magnetoresistance effects.[2−4] The parent compound $LaMnO_3$ is an antiferromagnetic insulator in which an orbital ordering is established by means of the cooperative Jahn-Teller effect breaking the degeneracy of the electronic configuration of Mn^{3+} ($t_{2g}^3\ e_g^1$).[5] This order seems to be responsible for an orthorhombic to rhombohedral phase transition at about 873 K which is similar to other structural transitions that take place at elevated temperatures in some related systems.[6,7] It was previously reported[8] that as the orthorhombic (space group *Pbnm*) distortion of the perovskite arrangement decreases, the rare-earth, O1 and O2 atoms approach the ideal positions at (0 0 1/4), (0 1/2 1/4) and (1/4 1/4 0), respectively.

We have recently reported some results on ionic conductors, especially in perovskites of general formula $Ln_{1.33-x}Na_{3x}Ti_2O_6$.[9−10] The partial substitution of titanium by manganese in these compounds could lead to mixed conductors showing high ionic and electronic conductivity. The measurement and control of mixed ionic-electronic conductivities has become recognized as being of technological importance in an increasing number of systems. Therefore, the aim of this paper is to report both the structural and electrical behaviors of $La_{1.33}Na_xMn_xTi_{2-x}O_6$ ($0.66 \geq x \geq 0.44$). A detailed investigation of the phase $La_{1.33}Na_{0.66}Mn_{0.66}Ti_{1.34}O_6$ has been undertaken in order to clarify the parameters controlling the crystal structure of this material. An orthorhombic to rhombohedral transition was found as in $LaMnO_3$. Nevertheless, the orthorhombic space group is different, *Ibmm*, and only a rhombohedral symmetry, $R\bar{3}c$, was found for the remaining compositions. Conductivity measurements were performed and the results are interpreted on the basis of the compositional features.

Results and Discussion

For the series $La_{1.33}Na_xMn_xTi_{2-x}O_6$, pure phases were found in the compositional domain $0.66 \leq x \leq 0.44$. All samples have the characteristic X-ray diffraction patterns of the perovskite structure, in which some reflections are split

Table 1. *R* factors agreement obtained in the refinements by XRD and ND

	XRD refinements (300K)			ND refinements (300K)		
Space group	R_P	R_{WP}	R_B	R_P	R_{WP}	R_B
$R\bar{3}c$	8.73	11.0	9.18	8.56	11.3	7.03
Pbnm	8.29	10.6	9.57	6.30	7.80	5.36
Ibmm	11.6	15.0	9.60	5.79	7.35	4.31

[a] Departamento de Química Inorgánica I,
Facultad de Ciencias Químicas, Universidad Complutense,
28040 Madrid, Spain
Fax: (internat.) + 34-91/394-4352
E-Mail: marisal@eucmax.sim.ucm.es

  1434−1948/00/0404−0659 $ 17.50+.50/0

indicating a noticeable distortion from the ideal cubic symmetry. For $x = 0.66$, the refinement was carried out in the rhombohedral space group $R\bar{3}c$, giving the unit cell parameters $a = 5.488$ Å and $c = 13.451$ Å; the R factors obtained in the refinement are gathered in Table 1.

On the other hand, an orthorhombic symmetry (whose parameters are related to the ideal perovskite ones as follows: $a_o \approx b_o \approx \sqrt{2}\, a_p$ and $c_o \approx 2\, a_p$) could be taken into account if we consider the Goldschmidt[11] factor, $t = [d(A-O)]/[\sqrt{2}\, d(B-O)]$, which is generally used as a tool for studying the perovskite structure. In our case, the value of $t = 0.97$, is compatible with an orthorhombic distortion. The XRD refinements were carried out in the space groups *Pbnm* and *Ibmm,* and the *R* factors obtained are included in Table 1. However these space groups give quite similar values and the results do not allow us to determine which is the more reliable structural model.

Neutron diffraction (ND) data were collected for the phase $La_{1.33}Na_{0.66}Mn_{0.66}Ti_{1.34}O_6$ in order to clarify the space group assignment. The *R* factors obtained by means of ND for the different space groups are also given in Table 1 and these results clearly suggest that the structure is accurately described in the *Ibmm* space group.

Neutron diffraction data were also collected for the same phase ($x = 0.66$) at different temperatures and were refined in an orthorhombic cell (space group *Ibmm*) at temperatures below 400 K that changes to a rhombohedral symmetry (space group $R\bar{3}c$) at higher temperatures (between 600 and 700 K).

The refined atom positions, lattice parameters and *R* factors obtained are listed in Table 2. The agreement between the observed and calculated integrated intensities of both orthorhombic and rhombohedral phases are considered as satisfactory with values of the crystal structure model indicators $R_B \leq 4.35$. The values of R_P and R_{WP} were ≤ 8.21 showing the reliability of the structure analysis.

Table 2. Refined Atomic Positions, Lattice Parameters, and R-factors for $La_{1.33}Na_{0.66}Mn_{0.66}Ti_{1.34}O_6$, obtained by neutron diffraction

		300 K	400 K	600 K	700 K
Space group		*Ibmm*	*Ibmm*	$R\bar{3}c$	$R\bar{3}c$
La/Na	*x*	−0.0042(4)	0.0062(8)	0.0000	0.0000
	y	0.0000	0.0000	0.0000	0.0000
	z	0.2500	0.2500	0.2500	0.2500
Mn/Ti	*x*	0.0000	0.0000	0.0000	0.0000
	y	0.5000	0.5000	0.0000	0.0000
	z	0.0000	0.0000	0.0000	0.0000
O1	*x*	0.0481(6)	0.0477(1)	0.4695(3)	0.4724(5)
	y	0.5000	0.5000	0.0000	0.0000
	z	0.2500	0.2500	0.2500	0.2500
O2	*x*	0.7500	0.7500		
	y	0.2500	0.2500		
	z	0.0214(6)	0.0197(1)		
a (Å)		5.4881(3)	5.4931(4)	5.5055(2)	5.5180(3)
b (Å)		5.4757(2)	5.4821(8)		
c (Å)		7.7407(7)	7.7501(1)	13.4618(1)	13.4844(1)
R_B (%)		4.35	4.21	4.20	4.14
R_P (%)		5.79	6.55	5.73	5.98
R_{WP} (%)		7.36	8.21	7.32	7.67

To illustrate graphically the matches between the complete observed and calculated data, neutron diffraction patterns and difference plots for the orthorhombic (300 K) and the rhombohedral (700 K) forms of $La_{1.33}Na_{0.66}Mn_{0.66}Ti_{1.34}O_6$ are plotted in Figures 1a and 1b, respectively. We will discuss the main characteristic features of both structures separately.

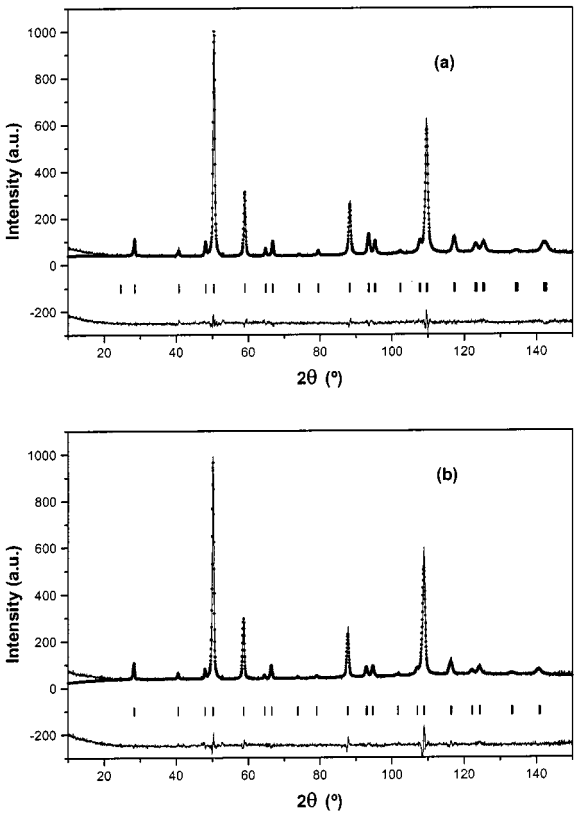

Figure 1. Calculated (full line) and observed (dots) ND patterns and difference spectrum for $La_{1.33}Na_{0.66}Mn_{0.66}Ti_{1.34}O_6$: (a) orthorhombic (300 K) and (b) rhombohedral (700 K)

Orthorhombic $La_{1.33}Na_{0.66}Mn_{0.66}Ti_{1.34}O_6$

The room temperature phase was refined in the orthorhombic space group *Ibmm*. Previous fits of the experimental results in the space group *Pbnm*, that frequently appears in orthorhombic perovskites, give higher *R* factors. In the inner-centered unit cell the Mn and Ti atoms are fixed at the 4b sites, and the La and Na atoms are located at the 4e, the O1 at the 4e and the O2 atoms at the 8g sites. The structure refinement for the title compounds, obtained separately from XRD and ND, are in good agreement and for the remaining compositions only XRD results will be discussed. An examination of the refined atomic coordinates, listed in Table 2, shows that Mn and Ti are placed on the ideal sites and the other atoms are only slightly displaced from their respective ideal positions. A comparison of the atomic coordinates obtained at 300 and 400 K shows that La, Na, O1 and O2 atoms remain nearly unchanged with temperature. Cations in the A-perovskite sites (La/Na) and

Table 3. Interatomic distances (Å) and angles (°) for BO_6 and AO_{12} polyhedra in $La_{1.33}Na_{0.66}Mn_{0.66}Ti_{1.34}O_6$, obtained by neutron diffraction

	300 K	400 K	600 K	700 K
d(Mn/Ti−O1)	1.953(5) (x2)	1.955(3) (x2)	1.951(1) (x2) 1.952(6) (x2)	1.954(8) (x4)
d(Mn/Ti−O2)	1.945(3) (x4)	1.946(1) (x4)	1.954(4) (x2)	1.956(9) (x2)
Mean	1.948	1.949	1.952	1.955
Shannon	2.018	2.018	2.018	2.018
O1−Mn/Ti−O2	89.3(8) (x4) 90.6(1) (x4)	89.0(5) (x4) 91.0(3) (x4)	89.7(8) (x4) 89.8(5) (x2)	89.7(5) (x4) 89.8(7) (x2)
O2−Mn/Ti−O2	89.4(4) (x2) 90.5(2) (x2)	89.5(7) (x2) 90.5(2) (x2)	90.2(3) (x2) 90.3(3) (x4)	90.2(2) (x2) 90.3(6) (x4)
Mn/Ti−O1−Mn/Ti	164.5(4)	164.5(6)		
Mn/Ti−O2−Mn/Ti	170.2(5)	171.0(9)	170.1(2)	171.1(9)
Mean	167.3	167.8	170.1	171.1
La/Na−O1	2.457(6) 2.748(4) (x2) 3.031(2)	2.450(2) 2.750(3) (x2) 3.042(4)	2.581(2) 2.585(1) (x2) 2.754(5) (x4) 2.755(1) (x2)	2.603(1) 2.607(3) (x2) 2.758(2) (x4) 2.759(3) (x2)
La/Na−O2	2.636(1) (x4) 2.847(3) (x4)	2.654(5) (x4) 2.835(6) (x4)	2.755(1) (x2) 2.917(6) 2.921(3) (x2)	2.759(3) (x2) 2.907(2) 2.911(3) (x2)
Mean	2.743	2.746	2.753	2.758
Shannon	2.772	2.772	2.772	2.772

in the B ones (Mn/Ti) will be noted in the following discussion as A and B, respectively.

To study the distortion around the Mn and Ti atoms which are in a BO_6 octahedral coordination, the interatomic distances, O−B−O angles and standard deviations have been calculated and are listed in Table 3. There are two different B−O sets of bond lengths in the octahedra, the average of which scarcely varies (from 1.948 to 1.949 Å) with increasing temperature. The average B−O distances are in good agreement with the sum of the Shannon ionic radii.[12] There are four different O−B−O angles with small deviations from the ideal 90° angle for a cubic perovskite. As can be seen from the interatomic distances and angles, the distortion within the BO_6 octahedron is rather small and the values are closer to ideal ones.

The orthorhombic distortion with respect to a cubic structure can be viewed as the BO_6 octahedra having faces tilted towards or away from each other and therefore the values of the B−O−B angles can be used to study the octahedra tilting. As shown in Table 3, the B−O1−B and B−O2−B angles for the orthorhombic phase $La_{1.33}Na_{0.66}Mn_{0.66}Ti_{1.34}O_6$ are significantly different from 180°, which is the expected value for an ideal cubic perovskite, and the octahedra tilting is ≈12.5°.

Lanthanum and sodium are located in the A sites and inside a twelve-coordinated polyhedron; the respective values of the A−O interatomic distances are gathered in Table 3. In comparison with those of the BO_6 octahedra, the A−O bond lengths vary over a wide range, indicating that these later polyhedra are quite distorted. An inspection of the twelve interatomic distances does not show any discontinuity in the increasing distances, and a division between the eight first-nearest and the four second-nearest oxygen atoms cannot be made, suggesting that it would be a good approximation to assign coordination number 12 to La and Na. The mean A−O distances are of the same order as the Shannon ones.

Rhombohedral $La_{1.33}Na_{0.66}Mn_{0.66}Ti_{1.34}O_6$

The high temperature phase is described as rhombohedral in the space group $R\bar{3}c$. From the hexagonal axes of reference, the A and B atoms are fixed at the 6a and 6b sites, respectively, and the O atoms are located at the 18e ones. The refined atomic coordinates, listed in Table 2, show that only the O atoms are slightly displaced from the ideal positions (1/2 0 1/4) with $\Delta x \approx 0.03$. The refined lattice parameters referring to hexagonal cell coordinates are also given in Table 2 (columns 600 and 700 K), the actual displacement of the O atoms from the ideal positions being about 0.16 Å. The respective values of the rhombohedral unit cell parameters, a_R and α_R, are 5.4990 Å and 60.08° (at 600 K) and 5.5093 Å and 60.10° (at 700 K), respectively.

The refined interatomic distances and angles of the BO_6 octahedron for this high temperature phase are also listed in Table 3, and show that each B atom is surrounded by six almost equidistant O atoms. The O−B−O angles are slightly deviated (± 0.3°) from the ideal value of 90° indicating that the distortion within a BO_6 octahedron is very small. However, the B−O−B angles are significantly different from the ideal angle of 180°, showing that octahedral tiltings remain in the rhombohedral phase. A structural model is depicted in Figure 2, in which the slight nonlinearity of the B−O−B bonds, which are deviated by around 10°, is denoted by the full lines.

The rhombohedral distortion can be viewed as being derived from a rotation of the BO_6 octahedra around the

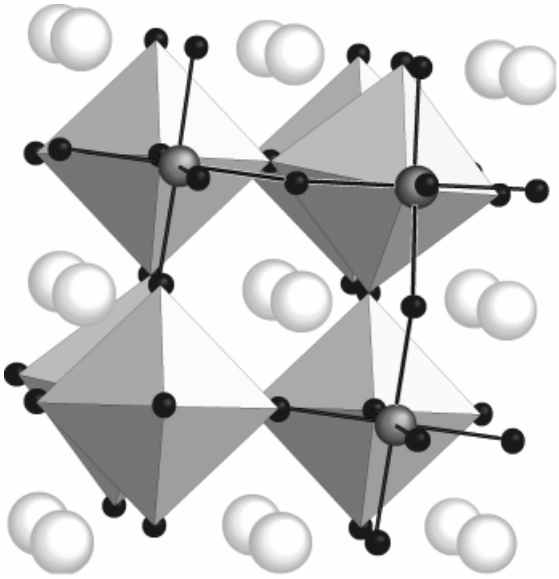

Figure 2. Structural model for compounds with rhombohedral symmetry

three-fold axis by an angle ω from the ideal perovskite position. The angle of rotation ω may be calculated from the oxygen position using $x = (\sqrt{3} - \text{tg}\ \omega)/\sqrt{12}$. The values of ω calculated at 600 and 700 K are 6.03° and 5.46°, respectively. There are different types of A−O distances for the rhombohedral phase of $La_{1.33}Na_{0.66}Mn_{0.66}Ti_{1.34}O_6$. In the absence of a sharp discontinuity in the increasing A−O distances we have assigned a coordination number 12 for the oxygen distorted polyhedra around these A atoms.

As stated above, the phase $LaMnO_3$ shows a cooperative Jahn-Teller effect that seems to be responsible for the orthorhombic to rhombohedral phase transition. Nevertheless, in our material ($x = 0.66$) only a third of the octahedral B-sites are effectively occupied by Mn^{3+}, with Ti^{4+} in the remaining ones, and any cooperative distortion must be excluded. This fact is supported by the similar B−O bond lengths that were encountered. Moreover, in the following phases ($x = 0.55$ and 0.44) only a rhombohedral symmetry appears in the whole range of temperatures studied, and therefore the adoption of such a symmetry in these systems with lower Mn^{3+} content cannot be attributed to a cooperative Jahn-Teller effect.

Rhombohedral $La_{1.33}Na_{0.55}Mn_{0.55}Ti_{1.45}O_6$ and $La_{1.33}Na_{0.44}Mn_{0.44}Ti_{1.56}O_6$

X-ray diffraction data for the phases $x = 0.55$ and 0.44, were tentatively refined on the basis of the space groups *Pbnm* and *Ibmm,* but the best fits were found in a rhombohedral symmetry (space group $R\bar{3}c$). Table 4 gathers the crystal parameters and *R* factors obtained for these compounds and a plot of the final observed, calculated and difference profiles is given in Figure 3 (for the composition $x = 0.44$). The agreements between profiles and *R* factors seem to confirm the validity of the proposed structural model. The basic features of the rhombohedral phases have been confirmed, and the results may be compared with those obtained in our neutron diffraction study.

Table 4. Refined atomic positions, lattice parameters and *R* factors for $La_{1.33}Na_xMn_xTi_{2-x}O_6$ ($x = 0.55$ and 0.44)

		$x = 0.55$	$x = 0.44$
Space group		$R\bar{3}c$	$R\bar{3}c$
La/Na	x	0.000	0.000
	y	0.000	0.000
	z	0.250	0.250
Mn/Ti	x	0.000	0.000
	y	0.000	0.000
	z	0.000	0.000
O1	x	0.462(1)	0.467(8)
	y	0.000	0.000
	z	0.250	0.250
a (Å)		5.493(6)	5.490(1)
c (Å)		13.444(6)	13.434(5)
R_B (%)		7.28	6.74
R_P (%)		7.94	8.57
R_{WP} (%)		10.6	11.2

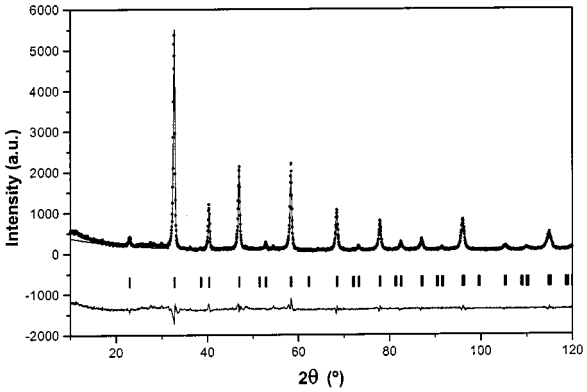

Figure 3. Calculated (full line) and observed (dots) XRD patterns and difference spectrum for $La_{1.33}Na_{0.44}Mn_{0.44}Ti_{1.56}O_6$ (rhombohedral)

On this basis, no differences in B−O bond lengths are encountered (1.952 Å for $x = 0.55$ and 1.948 Å for $x = 0.44$) and all the octahedra are regular. In consequence, the possible presence of a cooperative Jahn-Teller distortion, if it exists at a local level in the MnO_6 octahedra, is undetectable in the structure.

Electrical Properties

Measurements of a.c. impedance spectra have been carried out by alternating current techniques from the complex impedance (Z) plots. Experimental graphs at various temperatures show a semicircle and a spike. An apparent change in the nature of the charge carriers take place from electronic to electronic-ionic mixed conductors when x decreases, and this fact seems to be related to the higher number of cation vacancies in the structure.

Figure 4 shows the Z'' (imaginary part) vs. Z' (real part) plots for $x = 0.66$ at 300 and 326 K; it can be seen that the semicircle is somewhat depressed at this latter temperature.

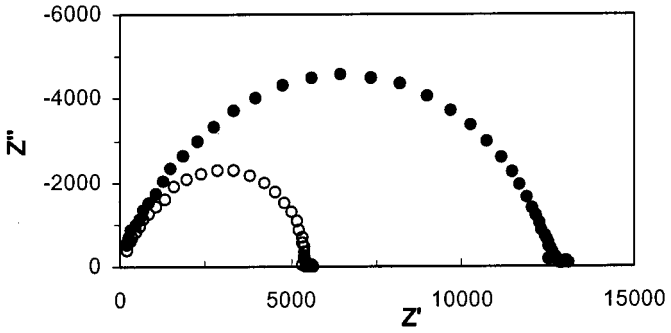

Figure 4. Complex impedance plots at 300 and 326 K for $La_{1.33}Na_{0.66}Mn_{0.66}Ti_{1.34}O_6$

However, for the samples $La_{1.33}Na_{0.55}Mn_{0.55}Ti_{1.45}O_6$ and $La_{1.33}Na_{0.44}Mn_{0.44}Ti_{1.56}O_6$ at temperatures between 298 and 333 K, a semicircle and a spike at low frequencies which is inclined by about 40° with respect to the Z′ axis were observed, and these could be associated with an electrode-electrolyte response (Figure 5, for $x = 0.55$).

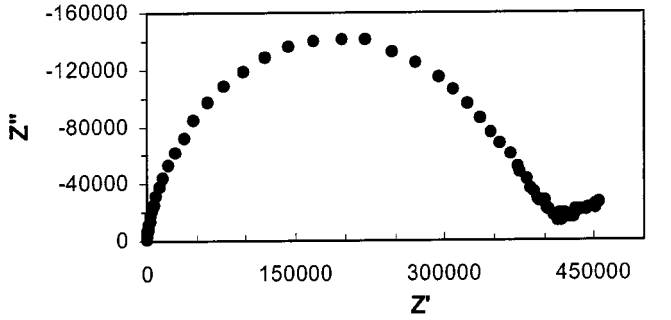

Figure 5. Complex impedance plots at 313 K for $La_{1.33}Na_{0.55}Mn_{0.55}Ti_{1.45}O_6$

Conductivity values for all samples were determined from the complex impedance plots over a wide range of temperatures and they can be fitted to an Arrhenius equation of the form: $\sigma = \sigma_o \times \exp(-Ea/kT)$. Figure 6 shows the linear plots of log σ vs. 1000/T for the three compositions. Conductivity values decrease with decreasing x, this fact being related to the total number of mobile sodium cations in the structure, although the respective activation energies remain almost constant.

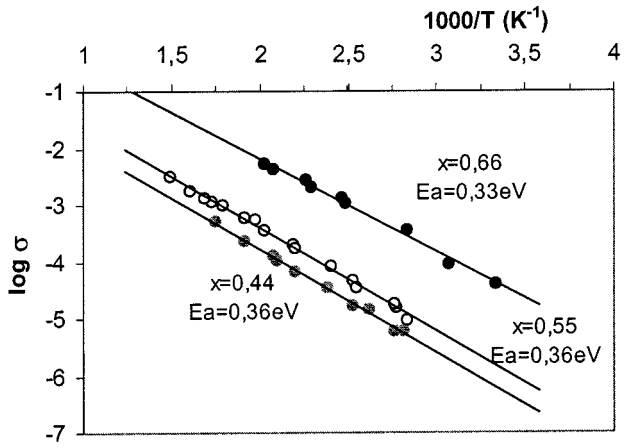

Figure 6. Arrhenius plots for the system $La_{1.33}Na_xMn_xTi_{2-x}O_6$

Charge/discharge experiments on cells consisting of pellets sandwiched between blocking platinum electrodes, showed that significant amounts of current could be passed on the charging cycle but another considerable amount is also detected on subsequently placing the cell in the discharge mode.[13] This phenomenon suggests that the products of charging were stored in the vicinity of the electrodes and were subsequently recovered on discharge, thereby indicating that a certain amount of ionic conduction occurs.

For purely ionic transport, where all the charge passed is stored and released on discharging, the ratio Q_d/Q_c (where Q_d and Q_c are the quantities of charge passed on the discharging and charging mode, respectively) should have the ideal value of unity. In a mixed ionic/electronic conductor, this ratio gives an approximate estimation of the ionic transport number, if one assumes that the reactions occur at the electrode-electrolyte interface during charging. For

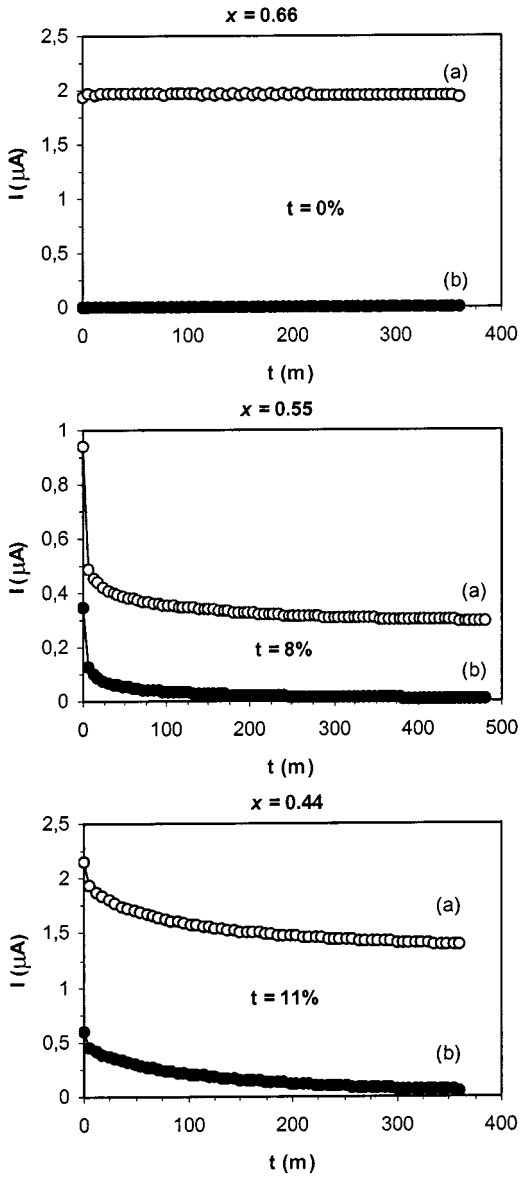

Figure 7. Current vs. time curves for charging/discharging for $x = 0.66$, 0.55 and 0.44 at 313 K (a) charging (b) discharging

purely electronic transport, the discharge current should be zero and the ratio Q_d/Q_c must also be zero. The following results of charging/discharging experiments have been interpreted in terms of these hypotheses.

The experimental results of charge/discharge processes at 313 K for all compositions are summarized in Table 5, and the respective curves are shown in Figure 7. The total charge passed through the system was calculated from the area under the I vs. t curves.

Table 5. Results of charging/discharging experiments at 313 K for $La_{1.33}Na_xMn_xTi_{2-x}O_6$

Composition	Q_c (C)[a]	Q_d (C)[b]	$t \approx Q_d/Q_c$[c]
0.66	7.04×10^{-4}	1.08×10^{-7}	1.53×10^{-4}
0.55	1.61×10^{-4}	1.29×10^{-5}	8.05×10^{-2}
0.44	5.53×10^{-4}	6.04×10^{-5}	1.09×10^{-1}

[a] Amount of charge passed during charging mode. – [b] Amount of charge recovered during discharging mode. – [c] Ionic transport number.

These results seem to confirm the different electric behavior of the materials as a function of their composition. The sample $x = 0.66$ (in which La and Na cations occupy all the A sites in the perovskite structure) behaves as a purely electronic conductor because ionic contribution is hindered. The samples $x = 0.55$ and 0.44 possess a relatively low number of A vacancies to which Na cations can move, and they show a mixed electronic-ionic conduction behavior.

Conclusion

In order to investigate materials with mixed ionic-electronic properties for their use as electrodes in solid-state batteries, some phases of general composition $La_{1.33}Na_x$-$Mn_xTi_{2-x}O_6$ have been obtained. From neutron powder diffraction data a structural transition between the orthorhombic (space group *Ibmm*) and rhombohedral (space group $R\bar{3}c$) symmetries is seen for $x = 0.66$. A similar transition from *Pbnm* to $R\bar{3}c$ symmetry is known for $LaMnO_3$ which is accompanied by an increase in the coordination number of A-cations from 8 to 12. In this respect, the space group *Ibmm* can be considered as a distorted intermediate that maintains the higher coordination number but shows a wide range of A–O bond lengths. The phases $x = 0.55$ and 0.44 adopt the rhombohedral $R\bar{3}c$ symmetry in which the BO_6 octahedra are clearly isolated and do not show any cooperative Jahn-Teller distortion.

All these phases behave as good conductors, on the basis of the relatively low activation energies, and, bearing in mind the absence of vacancies in the A sites when $x = 0.66$, this phase is a pure electronic conductor. The charge/discharge results can be interpreted as a function of the structural features.

Experimental Section

General Remarks: Polycrystalline samples of general composition $La_{1.33}Na_xMn_xTi_{2-x}O_6$ ($x = 0.66$, 0.55 and 0.44) were prepared by a classical ceramic method, from powdered mixtures of La(NO3)3·6H2O, $NaNO_3$, $C_{15}H_{21}MnO_6$ [manganese(III) acetylacetonate] and $C_{10}H_{14}O_5Ti$ (titanyl acetylacetonate), in a stoichiometric ratio, at 973 K for several days.

X-ray diffraction patterns were recorded with a Philips X′Pert-MPD diffractometer and a PW 3050/00 goniometer, using Ni-filtered Cu-K_α radiation and 2θ step size of 0.05°, with a counting time of 12.5 s for each step. The goniometer was connected to a PC controlled by the commercial program PC-APD (Analytical Powder Diffraction Software, 4.0).

The neutron powder diffraction data were recorded at four different temperatures on the D1A high-resolution powder diffractometer ($\lambda = 1.9110$ Å) at the Institut Laue-Langevin (Grenoble, France). The neutron and X-ray diffraction patterns were analyzed through the Rietveld method by the Fullprof program.[14] A pseudo-Voigt function was chosen to generate the line-shape of the diffraction peaks.

Electrical measurements were carried out with a Solartron 1260 Impedance/Gain Phase Analyzer with a frequency range of 0.1 Hz – 10 MHz. Samples were pressed into pellets and then sintered in air at 973 K for 48 h. Blocking electrodes were deposited on two faces of the pellets with platinum paint.

Polarization experiments in dc were carried out at 313 K with a charging voltage of 1 V for the compositions $x = 0.66$, 0.55 and 0.44. These samples and electrodes were the same as those used for conductivity measurements. The equipment includes a standard resistor that was in series with the sample during the charging and discharging cycles.

Acknowledgments

We are indebted to the CICYT (MAT 97–0326-C04–03) for financial support. We acknowledge the ILL for collecting data of ND. One of the authors (A.I.R.) is grateful to the C.A.M. for a grant.

[1] A. Atkinson, *Adv. Ceram.* **1987**, 23, 3.
[2] R. von Helmoth, J. Wecker, B. Holzapfel, L. Schulltz, K. Samwer *Phys. Rev. Lett.* **1993**, 71, 2331.
[3] Y. Tokura, A. Urushibara, Y. Moritomo, T. Arima, A. Asamitsu, G. Kido, N. Furukawa *J. Phys. Soc. Jpn.* **1994**, 63, 3931.
[4] S. Jin, M. McCormack, T. H. Tiefel, R. Ramesh *J. Appl. Phys.* **1994**, 76, 6929.
[5] J. Rodriguez-Carvajal, M. Hennion, F. Moussa, A. H. Moudden *Phys. Rev.* **1998**, B57, R3189.
[6] M. Marezio, J. P. Remeika, P. D. Dernier *Acta Cryst.* **1970**, B26, 2008.
[7] M. Marezio, P. D. Dernier, J. P. Remeika *J. Solid State Chem.* **1972**, 4, 11.
[8] T. C. Huang, W. Parrish, H. Toraya, P. Lacorre, J. B. Torrance *Mat. Res. Bull.* **1990**, 25, 1091.
[9] A. I. Ruiz, M. L. López, M. L. Veiga, C. Pico *Solid St. Ionics* **1998**, 112, 291.
[10] M. A. Arillo, J. Gómez, M. L. López, C. Pico, M. L. Veiga *Solid St. Ionics* **1997**, 95, 241.
[11] V. M. Goldschmidt, *Skr. Nor. Vidensk. Akad.*, Oslo, **1926**, 2.
[12] R. D. Shannon, *Acta Cryst.* **1976**, A32, 751.
[13] H. H. Sumathipala, M. A. K. L. Dissanayake, A. R. West *Solid St. Ionics* **1996**, 86–88, 719.
[14] J. Rodriguez Carvajal, *FULLPROF.* XV Congress of International Union of Crystallography, Toulouse **1990**, p 127, **1994** (Revised version).

Received March 19, 1999
[I99108]